Theranostic Radiopharmaceuticals

Subjects: Radiology, Nuclear Medicine & Medical Imaging | Physics, Nuclear | Chemistry, Medicinal

Contributor: Holis Holik, Faisal Ibrahim, Angela Elaine, Arifudin Achmad, Achmad Hussein Kartamihardja

Theranostic Radiopharmaceuticals (Radiotheranostics) is a term in the medical field to define the combination of therapeutic and diagnostic techniques by a suitable radiopharmaceutical agent. Radionuclides are isotopes that emit radiation or have excess nuclear energy, making them chemically unstable and tend to change into another atom. Various types of radiation can be emitted by radionuclides e.g. alpha particles, beta particles, and gamma energy. In radiotheranostics, a pharmaceutical agent (drug) is needed to be a carrier molecule that introduces the radionuclide to its target. Radionuclides are then used as a source of radiation in radiotheranostics that are responsible for diagnosing or treating various diseases.

Keywords: radiopharmaceuticals ; theranostics ; radionuclide ; chelator

1. Radionuclides for Diagnosis Purposes

SPECT and PET have become increasingly popular cancer imaging techniques. The radiopharmaceuticals use a gamma (γ) or beta (β^+) emitted radionuclide to selectively interact with a target tissue. In PET and SPECT tracers, a variety of radionuclides have been utilized, including isotopes ranging from ^{11}C ($t_{1/2}$= 20 min) to ^{124}I ($t_{1/2}$= 4.2 days), as shown in **Table 1** [1].

In the PET scan, the annihilation of positron caused by the collision between positron and electron in the body generates gamma rays in two opposite directions which can be detected by the PET scanner to build a radiogram. The acceptable resolution of radiopharmaceuticals should be about ~5 mm. The position of annihilation (collision) varies between the different radionuclides, this is the reason behind the various resolution of the radiogram for each radiopharmaceutical. For example, a positron released by ^{18}F (E+ = 250 keV) travels 1 mm before being annihilated, but a positron emitted by ^{68}Ga (E+ = 830 keV) travels 35 mm before being annihilated. As a result, PET pictures acquired with ^{68}Ga have poorer resolution than those produced with ^{18}F [2][3].

On the other hand, SPECT uses the gamma rays produced by a radioactive isotope to be further screened by the device. Because gamma rays are solitary events, unlike annihilation photons, they must be detected by putting a lead collimator between the source and the detector which then provides information about each source of radiation in the cell of interest [4]. Any photons that interact with the detector must have come from a parrarel source to the detector's face. The energy of the photon being photographed is an essential factor to consider. Low-energy photons (~70 keV) are strongly attenuated by tissue, resulting in distortions in the pictures. If the photon energy is too great, the demand for similarly thick collimators becomes prohibitive. Photon energies of the order of 140 keV are predicted from these two variables, indicating that ^{99m}Tc is widely used for SPECT diagnosis [5].

Table 1. Radionuclides for diagnosis purposes.

Radionuclide	Half-Life	Mode of Decay	Energy (KeV) (%Abundance)	Indication (in Radiopharmaceutical Form)	References
^{99m}Tc	6.02 h	γ	140.5 (89%)	(*I,I*-[^{99m}Tc]Tc-ECD) Functional imaging of the brain *, [99m Tc-MDP] bone scintigraphy *	[6][7][8]
^{111}In	67.3 h	EC	171 (90%) 295 (94%)	(^{111}In-pentetreotide) imaging of neuroendocrine tumors *, (Capromab Pendetide) for metastatic prostate cancer *, and leukocyte marking for invitro purposes *	[9][10][11][12][13]
^{18}F	109.7 min	β^+ EC	635 (97%) 1655 (EC) 3%	FDGPET radionuclide for cancer * and Piflufolastat PET radionuclide for protate cancer imaging *	[14][15]

Radionuclide	Half-Life	Mode of Decay	Energy (KeV) (%Abundance)	Indication (in Radiopharmaceutical Form)	References
^{11}C	20.4 min	β^+	960 (100%)	Imaging of tyrosine kinase receptor *****, [^{11}C]Flumazenil for GABA **** imaging, [^{11}C]mZIENT for imaging serotonin receptor *****, and 11C-coenzyme Q10 myocardial imaging *****	[16][17]
^{133}Xe	5.27 days	γ	81 (38%)	Cerebral blood flow, Xe Technegas for lung perfusion imaging **	[18][19]
^{201}Tl	73 h	γ	135 and 167	imaging of soft tissue and bone tumors, detection of recurrence in gliomas	[20]
^{51}Cr	27.7 days	γ	320 (9.8%)	Red blood cell labeling, 51-EDTA for GFR measurement ***	[21][22]
^{67}Ga	78.3 h	EC γ	EC (100%) γ (93 (39%), 300 (17%), and 185 (21%))	Imaging skeletal infection, ^{67}Ga–Citrate for CSF flow imaging ****	[23][24][25]
^{68}Ga	68 min	β^+	890 (90%)	Diagnosis or imaging of myocardial perfusion use Ga-68 Galmydar ****, pulmonary perfusion ****, and PSMA for prostate cancer *.	[26][27]
^{123}I	13 h	EC	159	Ioflupane I-123 Injection * Injection Dopamine transporter for parkinson's diagnosis	[28][29]
^{125}I	59.4–60.2 d	EC	28.5	Evaluation of glomerular filtration rate and imaging of thyroid, and 125 Iodine Seeds for brachytherapy in solid tumor *.	[30][31][32][33][34]
^{82}Rb	75 s	β^+	776	$^{82}Rb(Rb)^+$**** for myocardial ischemia and brain tumors imaging.	[35][36]
^{13}N	9.97 min	β^+	492 (100%)	^{13}N-ammonia * for myocardial perfusion and blood flow imaging in tissue.	[37]
^{166}Ho	26.8 h	β^- γ	1.774 (50%) 80.57 (6.6%)	^{166}Ho-chitosan ***** for diagnosis of liver cancer	[38][39]
^{89}Zr	78.4 h	β^+	395 (23%)	Diagnosis of various types of tumor and cancer (pancreatic, lymphoma, liver, colorectal, and prostate) (^{89}Zr-trastuzumab, ^{89}Zr-J951, ^{89}Zr-lumretuzumab) *****	[40]
^{61}Cu	3.3 h	β^+ EC γ	1220, 1150 (62%); 940, 560 (38%); 380 γ (3%)	^{61}Cu-ATSM ***** imaging of tumor hypoxia.	[41]
^{64}Cu	12.7 h	β^+ β^- γ	657 (19%), 141 (38%) 511 (43%),	^{64}Cu-SAR-bisPSMA *** Imaging for prostate, ^{64}Cu-DOTA-Trastuzumab *** breast cancer, ^{64}Cu-ATSM *** diagnosis of cervical cancer, ^{64}Cu-DOTA-Daratumumab **** multiple myeloma, and ^{64}Cu-Cl_2 urological malignancy.	[42][43]

Note: * FDA approved. ** Clinical trial phase III. *** Clinical trial phase II. **** Clinical trial Phase I. ***** Pre-clinical Studies.

a. ^{99m}-Technetium

^{99m}Tc ($t_{1/2}$ = 6,02 h, E = 140.5 keV (89%)) is widely used for SPECT, with ^{99m}Tc radiopharmaceuticals accounting for more than 85% of all nuclear medicine studies [44]. The emission and half time of ^{99m}Tc are almost ideal for convenient preparation of radiopharmaceuticals and imaging applications [45]. Several in vitro studies regarding the toxicity of ^{99m}Tc have been performed. The results of studies showed that [^{99m}Tc]TcO_4^- was able to induce DNA damage in breast cancer epithelial cells and reduce cell survival rate when the [^{99}m-Tc]TcO_4^- was transported into cells. About 30 mBq/cell of cellular concentration of ^{99}m-Tc was required to reduce the survival rate to 37%. Currently, ^{99m}Tc is widely used as a radiodiagnostic agent because it has several advantages e.g., widely available, can produce a variety of complexes with desired characteristics due to multi-oxidation state, sufficient half-life (6.02 h) for the preparation of ^{99m}Tc radiopharmaceuticals (in hospitals or centralized radiopharmacies), and decays into ^{99}Tc which has low toxicity (weak beta emission and very long half-life) [45][46][47].

^{99m}Tc has traditionally been generated via a ^{99}Mo/ ^{99m}Tc generator using parent ^{99}Mo created by the fission of highly enriched ^{235}U. The ^{99}Mo is separated from the $^{99}MoO_4^{2-}$ and immobilized through the alumina column [46]. By eluting the generator with 0.9% (isotonic) saline solution, ^{99m}Tc is produced as ^{99m}Tc O_4^-. Schaffer et al. demonstrated that a biomedical cyclotron could create 7.7 GBq (208 mCi) of ^{99m}Tc after 1.5 h of irradiation with an 18 MeV proton beam.

The primary distinctions between rhenium and technetium are their redox behaviors and kinetics. They are found in oxidation levels ranging from +7 to +1 and belong to the same group of transition metals (VIIB) as manganese. Tc(V) and Re(V) produce structurally similar complexes, but the formation circumstances and stability of the resultant products differ, with ^{188}Re complexes being easier to oxidize [47].

A reducing agent, most often $SnCl_2$, chelating (e.g., DTPA, DOTA, and SAR), and a buffer are usually included in a ^{99m}Tc kit. The ^{99m}Tc O_4^- solution in saline is simply injected into the vial to make the ^{99m}Tc complex [48][49]. Tc(V)-oxo or -dioxo (d^2) complexes are formed by reducing ^{99m}Tc O_4^- with $SnCl_2$, yielding square-pyramidal or octahedral complexes, respectively, with tetradentate having higher in vivo stability and simpler chemical modification, and so becoming the popular choice. Amido thioether thiol (AATT) and single amino acid chelate (SAAC) systems are examples of this tetradentate kind of complex [50].

b. ^{111}Indium

^{111}In ($t_{1/2}$ 2.8 d) is the most typical application for cell labeling, which has the advantage of being compatible with SPECT rather than with PET. For the tagging of a wide range of cell types, two compounds have proven especially useful: [^{111}In]In(oxinate)$_3$ and [^{111}In]In(tropolonate)$_3$ with In(oxinate)$_3$ have been the most used in clinic [1]. ^{111}In is a source of gamma radiation used for diagnosis, is also a source of low-energy auger electrons, and has a short distribution range. The presence of electrons outside the cell can be neglected, but when these electrons are inside the cell or around the cell nucleus, they can have a highly toxic effect on the cell's DNA. A comparative study of dosimetric estimation of ^{111}In showed that ^{111}In was transported into cancer cells in a cumulative concentration range of about 3.7–9.4 mGy/MBq, whereas in the liver ^{111}In had a cumulative concentration range of 0.6–0.4 mGy/MBq. The result of the study indicated that ^{111}In accumulates higher in cancer cells when compared to normal cells and can induce a cytotoxic effect against cancer cells [10].

Proton irradiation of enriched ^{112}Cd targets with the ^{112}Cd(p,2n)^{111}In reaction is the most frequent method for producing ^{111}In. At proton energy of approximately 25 MeV, this reaction can be performed in intermediate energy cyclotrons [50]. Indium, like gallium, has just one stable oxidation state in water: +3. However, due to its much greater size at 62–92 pm for ionic radius (4–8 Å), In(III) achieves coordination numbers of seven and even eight in its complexes. Indium complexes formed by the acyclic chelators EDTA and DTPA are highly thermodynamically stable. The hexadentate chelator in the seven-coordinate In-EDTA structure approximates a pentagonal bipyramidal geometry [51].

c. ^{67}Galium, and ^{68}Gallium

Gallium has a +3 oxidation state in an aqueous solution, which is comparable to ^{111}In. Ga^{3+} is a hard metal (small and highly charged cation) with an ionic radius of 4–6 CN (0.4–0.6 Å) that prefers to bind chelator with numerous anionic oxygen and/or nitrogen donor sites (e.g., DOTA, NOTA, and HBED) [52][53]. The variation of Ga^{3+} coordination number from 3 to 6 support octahedral complexes, the most common and the most stable Ga3+-based radiopharmaceuticals. pH sensitivity is a significant problem in Ga^{3+} labeling; gallium quickly hydrolyzes at pH>3, converting it to insoluble $Ga(OH)_3$. As a result, it is commonly labeled in acidic circumstances (pH 3–4), with the use of an intermediary ligand as an option (e.g., citrate or oxalate) [5][54].

Two radionuclides, ^{67}Ga and ^{68}Ga, have dominated the development of gallium-based radiopharmaceuticals. The low (γ) energy emitter ^{67}Ga ($t_{1/2}$ = 78.2 h) decays solely via electron capture (EC) [55][56]. Gallium-67 also generates high-energy (6.3 KeV) and long-range Auger electrons, which has spurred interest in ^{67}Ga for treatment purposes [57]. Gallium-67 is commonly made by bombarding a ^{nat}Zn or isotopically enriched ^{68}Zn target with the nuclear reactions ^{68}Zn(p,2n)^{67}Ga (photon energy range between 15 and 30 MeV) and/or ^{67}Zn (p,n)^{67}Ga (photon energy range between 10 and 20 MeV) and/or ^{67}Zn (p,n)^{67}Ga (photon energy range between 10 and 20 MeV [58].

^{68}Ga ($t_{1/2}$ = 67.7 min) on the other hand, is a (β^+) emitter (89%) with a mean (β^+) energy of 0.830 MeV, allowing it to be utilized for diagnostic imaging with PET. Gallium-68 is generated by the ^{nat}Ga (p,xn)^{68}Ge nuclear reaction, which is then absorbed on a column containing either an inorganic (e.g., TiO_2, Al_2O_3, and SnO_2) or organic (polymeric) stationary phase, and then eluted as $^{68}GaCl_3$ with 0.1–1 M HCl for further radiolabeling [59][60].

^{68}Ga and ^{111}In are used for inflammatory diagnosis and tumor imaging. Gallium(III) (Ga^{3+}) has comparable properties to Fe-III when in the body to bind to transferrin and lactoferrin and be transported to sites of inflammation. Compared with In(III), Gallium has advantages over indium in imaging osteomyelitis (bone infection) and chronic inflammation due to its ability to bind neutrophil cell membranes. In another utilization, ^{111}In is most suitable with peptides labeled for the somatostatin receptor and antibody receptor for prostate tumor imaging [61][62]. Several recent studies of cytotoxicity of ^{67}Ga have shown that ^{67}Ga caused DNA damage higher than ^{111}In per Bq concentration. The level of cellular radioactivity required by ^{67}Ga to kill 50–90% of breast cancer cells is 1.5–6 times less than ^{111}In. In addition, ^{67}Ga also has a lower level of DNA damage than ^{111}In if the radionuclide was separated from DNA, which caused ^{67}Ga to have a smaller DNA damage effect on non-targeted cells [25].

d. ^{61}Copper and ^{64}Copper

^{61}Cu is produced from the cyclotron (^{61}Ni(p,n)^{61}Cu) whereas ^{64}Cu is produced from ^{64}Ni(d,2n)^{64}Cu with γ emissions (43%) and produced from ^{64}Ni(p,n)^{64}Cu with β^+ emissions (19%). The half-life of ^{61}Cu is shorter than ^{64}Cu, making ^{64}Cu the most used for radiodiagnostic development due to its higher stability [63]. The coordination chemistry of copper, which is quite diverse ~4 to 6, makes Cu isotopes stably functional with BFCs. On the other hand, Cu has two states of oxidation, Cu(I) and Cu(II); thus, the complex remains stable and soluble with chelators phosphine-P and thioether-S (weak donor chelator). Because of the d9 configuration, Cu(II) complexes are more kinetically able to dissociate to ligands than Cu(I) with Cu(I) d10 configurations. Therefore, the compatible chelator Cu radionuclides are generally macrocyclic chelators, making Cu(II) complexes stably conjugated with the ligands [64][65]. The cytotoxicity study of ^{64}Cu radionuclide conjugated with carriers and chelators showed that the accumulated concentration of ^{64}Cu was 3.1–6.0 times higher in cancer cell models than in normal cell models. These results indicate higher efficiency of ^{64}Cu in cancer cells. The result shows that ^{64}Cu has the potential to be used as a radionuclide for cancer therapy or diagnosis [63].

e. ^{89}Zirconium

The half-life of Zr-89 ($t_{1/2}$ = 78.4 h) is the most suitable for antibody-based radiopharmaceuticals, due to their slow pharmacokinetics. It has relatively low positron energy (395 keV), which results in ideal radionuclides for PET with high-resolution imaging and is also more stable and safer in vivo. Hence, ^{89}Zr has more uses than ^{124}I-based agents for clinical applications. In addition, ^{124}I produces different energies, 723 keV (10.4%), 1691 keV (10.9%), and 603 keV (63.0%), which may lead random result to imaging. However, proper handling during high abundance production is necessary to lower the risk of high energy and penetrating photons (909 keV) [40].

f. ^{18}Fluorine

Despite the benefits of ^{68}Ga, such as its ability to be obtained from a generator or its metallic nature of molecules via coordination chemistry, ^{18}F continues to have a privileged position among the radionuclides used in PET imaging. The sensitivity and spatial resolution of ^{68}Ga PET imaging are lower than those of ^{18}F PET. With a bond strength of around 670 kJ/mol, aluminum forms more stable complexes with fluorine than with other halogens. Furthermore, because the Al-F bond is extremely stable in vivo, tiny quantities of the aluminum fluoride complex are compatible with organisms. With a maximum coordination number of six, the Al^{3+} ion can be complexed by an appropriate chelator and form a ternary complex (fluorine aluminum–chelator) in the presence of fluoride ions. If the ligand's valency permits it, it prefers to assume an octahedral geometry [66][67].

The relatively fast in vivo pharmacokinetics of peptide bioconjugates are consistent with the fluorine-18 half-life, making them ideal for [^{18}F]AlF radiolabeling. Good labeling yields of up to 74% have also been produced employing a NODA-MPAA-conjugate (IMP485), a pentavalent chelator better suited to [^{18}F]AlF, according to McBride, W.J et al. [68].

2. Radionuclides for Therapy Purposes

High-energy, short-range radiotherapy is thought to be adequately targeted the tumor tissue without inflicting considerable harm to normal tissue. Radiotherapy should have a high tumor-to-background ratio, be selective in its penetration, and be eliminated quickly by the kidneys. Radionuclides that primarily emit (β^-) particles, alpha particles, and/or Auger electrons have been used in medicinal radiopharmaceuticals thus far (**Table 2**) [69]. Auger electrons (mostly in ^{67}Ga) are extremely low-energy electrons (1–10 keV) produced by radionuclides decaying via electron capture. These particles have a high Linear energy transfer (LET) (4–26 keV/m) and a tissue range of less than a single cell diameter (1–20 m), making them ideal for nucleus targeting [70].

Table 2. Radionuclides for therapy purposes.

Radionuclide	Half-Life	Mode of Decay	Energy (KeV)	Indication (in Radiopharmaceutical Form)	References
^{90}Y	64.10 h	β^- β^+ γ	2270 (100%) 739 (0.003%) 511 (0.006%)	90Y-microsphere (TheraSphere® and SIR-Spheres®) * radiotherapy for hepatic metastasis, 90Y-ibritumomab tiuxetan ** for lymphoma, and ^{90}Y-hydroxypatite and ^{90}Y-citrate colloid ** for leukemia PVNS (synovitis).	[71][72]
^{117m}Sn	13.6 d	IT	130 150	^{117m}Sn-DTPA *** for bone tumor treatment and palliative therapy.	[71]
^{131}I	8.02 d	β^-; γ	606 (89.3%); 364 (81.2%)	^{131}I (radioactive iodine therapy) * use for therapy in thyroid cancer, for hyperthyroidism, RIT for NHL, and therapy for malignant pheochromocytoma neuroblastoma	[71][73]
^{153}Sm	46.5 h	β^-	808 (20%); 710 (50%)	^{153}Sm-EDTMP * for painful bone metastasis and synovitis tratment.	[71][72][74][75]
^{177}Lu	6.73 d	β^-	498 (78%)	^{177}Lu-HA **** for synovitis treatment, ^{177}Lu-PSMA-617 (Pluvicto) * for prostate cancer, ^{177}Lu-DOTATATE (Luthatera ®) * for neuroendocrine tumor.	[71][72]
^{225}Ac	10 d	α	5793 (18.1%) 5830 (50.7%)	^{225}Ac-PSMA-617 **** for prostate cancer, ^{225}Ac-lintuzumab *** for leukemia, and ^{225}Ac-NOTA-trastuzumab ***** for breast cancer treatment	[76]
^{186}Re	3.72 d	EC, β^-	1965 β^- (25.6%)	^{186}Re-HEDP *** for painful skeletal metastasis and painful arthritis	[71][72]
^{188}Re	17.00 h	β^-, γ	2120 (71.1%)	^{188}Re-HEDP *** for painful bone metastasis, rheumatoid arthritis, and treatments for RIT with various cancers	[71][72]
^{223}Ra	11.44 d	α	5979 (100%)	^{223}Ra-dichloride (Xofigo®) * for bone metastasis	[77]
^{166}Ho	26.8 h	β^- γ	1774 (49.9%) 80.57 (6.6%)	^{166}Ho-chitosan ***** for liver cancer	[39]

Note: * FDA approved. ** Clinical trial phase III. *** Clinical trial phase II. **** Clinical trial Phase I. ***** Pre-clinical Studies.

LET is a popular method for predicting the possible harm that a nuclide might produce in a biological system. Particles having a high LET generate ionizing radiation that quickly disperses in tissue. Particles having a low LET, on the other hand, attenuate their energy slowly, allowing them to deposit energy over a wider range of tissue.

a. ^{186}Rhenium and ^{188}Rhenium

^{188}Re has a half-life of about 17 h and emits β^- particles (2120.4 keV, 71.1%; and 1965.4 keV, 25.6%), while ^{186}Re has a longer $t_{1/2}$ (90 h) and emits (β^-) particles (1077 keV, 71%; and 939 keV, 22%) resulting in a longer tissue penetration (10–11 mm). Based on physical properties, ^{188}Re isotopes are excellent for radiotherapy of malignant tumors [78]. Some of the chemical properties of ^{186}Re and ^{186}Re are quite similar to ^{99}m-Tc because of their periodic linkage, but ^{186}Re and ^{188}Re have a lower redox state than ^{99}m-Tc, making them incompatible with several BFCA of ^{99}m-Tc. Ram et al. find the BFCA for peptide-based antibody which has a more stable complex for ^{99}m-Tc and ^{186}Re [79].

Based on phase II clinical trials and dosimetry tests of radiopharmaceuticals labeled with ^{188}Re, ^{188}Re-HEDP has effective pain relief in patients with breast or prostate cancer bone metastases (80% of 15 patients), lung cancer bone metastases (46% of 27 patients), renal cancer (50% of 61 patients), and liver cancer (55.56% of 64 patients). The dosimetry test of ^{188}Re-HEDP showed the maximum tolerated dose was 3.3 GBq, and the radiation-absorbed dose in normal bone marrow was still tolerable and did not cause hematological toxicity [79].

b. ^{225}Actinium

Actinium is present naturally in association with uranium. ^{225}Ac [$t_{1/2}$= 10 d; α emission 5793 keV (18.1%), 5830 keV (50.7%)] is derived from the decay of ^{233}U as well as the transmutation of neutron of ^{226}Ra by successive n, γ capture decay reactions via ^{227}Ac, ^{228}Th, and ^{229}Th. In the clinical trials, ^{225}Ac can be obtained from U.S. Department of Energy, Oak Ridge National Laboratory (ORNL) in Oak Ridge, TN, United States of America, and the Institute for Transuranium Elements in Karlsruhe, Germany. The ^{225}Ac from both places were produced from 233U and the long-term storage was done in ORNL [80].

^{225}Ac is an α emitter that has a recoil event (see **Figure 1**) as a challenge when it is complexed with a certain BFCA. There are broad techniques offered to deal with those problems; the first method is to use a nano-carrier capacity to hold the recoiling offspring, such as zeolites or liposomes. Piotrowska et al., 2013, utilized zeolites as transporters for ^{224}Ra and found that under circulating blood conditions, the fraction of recoiled daughters (^{212}Bi, ^{212}Pb, and ^{208}Tl) escaped from the zeolites is minimal [81]. The second strategy is to guarantee that the radiopharmaceutical is quickly absorbed by tumor cells and that any residual unabsorbed material is quickly eliminated from the body. Antibodies have received a lot more interest in the field of alpha radionuclide treatment. The third strategy is to place or inject alpha-emitting radionuclides directly into/near the tumor tissue, as Cordier et al. did in Phase I clinical trials using a radiopharmaceutical coded as "^{213}Bi-DOTA-substance P" which was locally injected in gliomas [82].

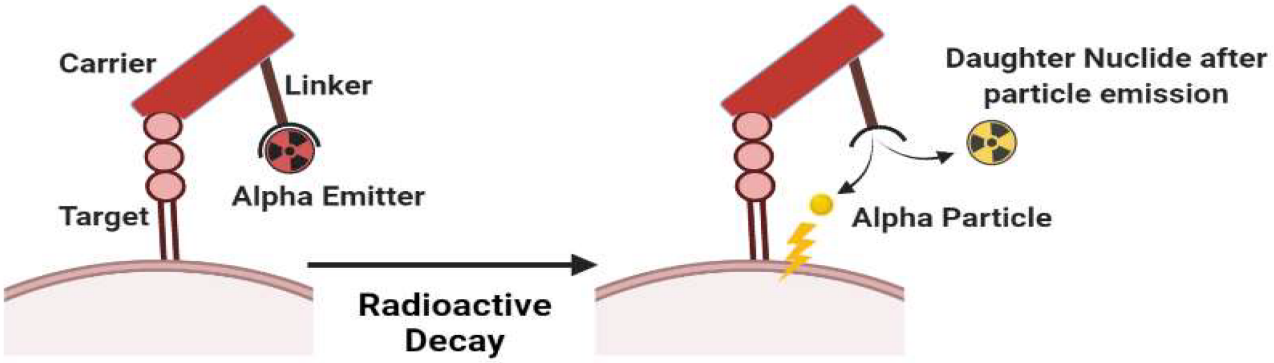

Figure 1. Scheme of complex instability of alpha emitter due to recoil energy effect.

c. ^{90}Yttrium

^{90}Y is in equilibrium with its parent isotope ^{90}Sr and then decays to form the stable ^{90}Z. ^{90}Y is formed from ^{89}Y being bombarded with neutrons in a nuclear reactor. ^{90}Y has a half-life of about 2.67 days and emits a large amount of β^- (2.27 MeV) and a little β^+ and γ emission, capable to penetrate tissues up to 11 mm. Due to the high energy β^- emission by ^{90}Y, the beta particle radiation not only reaches the target but also rapidly reaches the surroundings of the target cell. About 90% of the radiation is absorbed in a path length of 5 mm (about 100–200 cells). The ^{90}Y emitted beta particles can, directly and indirectly, disrupt cell integrity. Directly, beta particles will damage the DNA structure so that it cannot be repaired. Meanwhile, the emitted beta particles can increase the amount of toxic free radicals in the cytosol indirectly (known as a secondary radiation effect) [83][84].

^{90}Y is a good example of both medicinal and diagnostic isotopes being accessible in the same element. It has a lengthy half-life of 2.7 days, which is long enough to achieve radiotherapy's critical dosage levels. High energy causes the cell to penetrate deeply, which is ideal for solid tumors. Because of its larger tissue penetration range, ^{90}Y was predicted to have a bigger influence on tumor reduction [83].

The strong affinity of unchelated yttrium for bone and liver dominates the bioinorganic chemistry of Y^{3+}, which necessitates the employment of macrocycle chelators and emphasizes the importance of complex stability. Yttrium(III) is much bigger, having an ionic radius of 6–9 Å, giving it the ability to achieve coordination numbers of 7 and 10 in its complexes. The octadentate lanthanide chelator DOTA offers a nearly perfect match with associated high affinity due to the higher coordination number requirement of Y(III) [84][85].

Although (n,γ) reactions on yttrium metal or yttrium oxide can generate yttrium-90, the resultant product has a poor specific activity. It may also be made in a nuclear reactor by the ^{90}Zr(n,p)^{90}Y reaction. After irradiation, the Zr starting material is removed with HNO_3 and mandelic acid, yielding a solution comprising the ^{90}Y daughter and the ^{90}Sr parent, which may be removed from the ^{90}Y product by retaining it on a DOWEX cation column [85].

d. ^{177}Lutetium

In the application of radionuclide-based therapy, ^{177}Lu is now becoming the market leader. ^{177}Lu ($t_{1/2}$ = 6.7 d) is a β^- (0.497 MeV), γ (113 keV, 6%) and (208 keV, 10%) emitters. The development of ^{177}Lu to be a theranostic agent is very prospective, its utilities are not only a post-treatment scans be acquired, but patient dosimetry can also be performed [86][87]

In 2018, [^{177}Lu]Lu-DOTATATE (Lutathera) was approved by the FDA for use as a cancer treatment following a phase III clinical trial. Studies regarding PRRT combining [^{177}Lu]Lu-DOTATATE with [^{90}Y]Y-DOTATATE have shown that kidney

injury and myelosuppression are rare side effects. Hematotoxicity due to PRRT can occur due to irradiation and destruction of hematopoietic cells. The acceptable dose of PRRT for bone marrow is 2 Gy [88].

There are two methods of ^{117}Lu production, direct and indirect methods. The direct approach uses the ^{176}Lu(n,γ) ^{177}Lu nuclear reaction to irradiate highly enriched ^{176}Lu targets with neutrons. In the reaction ^{176}Yb(n, γ) ^{177}Yb → ^{177}Lu, the indirect approach employs highly enriched ^{176}Yb as a target material and needs chemical separation of ^{177}Lu from excess Yb [89]. Polycarboxylate ligands (DOTA, NOTA, NODAGA, DTPA, and DOTRP) have been demonstrated to be the most successful choice for developing a BFC capable of binding ^{177}Lu and producing a radioconjugate with adequate stability in an aqueous solution and under biological conditions for ^{177}Lu labeling. The chemical bonds produced by the Lu^{3+} ion have a strong ionic nature, requiring negatively charged hard donor elements such as oxygen for stable coordination. Negative oxygen atoms in polycarboxylate ligands appear to have a function in providing a strong ionic connection with the ionic metallic core. This is an important element in lowering the enthalpy of thermodynamically favorable processes [90].

e. ^{153}Samarium

^{153}Sm has physical properties being beta emission minus 0.71 MeV (50%) and 0.81 MeV (20%) and an emitted gamma emission 103.2 keV (28%). Beta particles from ^{153}Sm can penetrate soft tissue up to a maximum distance of 3 mm and can penetrate bone up to 1.7 mm, so it is used to reduce bone pain and bone loss due to cancer-causing illnesses and is also used for gamma imaging biodistribution [74][75].

References

1. MacPherson, D.S.; Fung, K.; Cook, B.E.; Francesconi, L.C.; Zeglis, B.M. A Brief Overview of Metal Complexes as Nucl ear Imaging Agents. Dalton Trans. 2019, 48, 14547–14565.
2. Rahmim, A.; Qi, J.; Sossi, V. Resolution Modeling in PET Imaging: Theory, Practice, Benefits, and Pitfalls: Resolution M odeling in PET Imaging. Med. Phys. 2013, 40, 064301.
3. Calais, J.; Kishan, A.U.; Cao, M.; Fendler, W.P.; Eiber, M.; Herrmann, K.; Ceci, F.; Reiter, R.E.; Rettig, M.B.; Hegde, J. V.; et al. Potential Impact of 68Ga-PSMA-11 PET/CT on the Planning of Definitive Radiation Therapy for Prostate Canc er. J. Nucl. Med. 2018, 59, 1714–1721.
4. Ljungberg, M.; Pretorius, P.H. SPECT/CT: An Update on Technological Developments and Clinical Applications. Br. J. R adiol. 2018, 91, 20160402.
5. Wadas, T.J.; Wong, E.H.; Weisman, G.R.; Anderson, C.J. Coordinating Radiometals of Copper, Gallium, Indium, Yttriu m, and Zirconium for PET and SPECT Imaging of Disease. Chem. Rev. 2010, 110, 2858–2902.
6. Boschi, A.; Uccelli, L.; Martini, P. A Picture of Modern Tc-99m Radiopharmaceuticals: Production, Chemistry, and Applic ations in Molecular Imaging. Appl. Sci. 2019, 9, 2526.
7. Rahmanian, N.; Hosseinimehr, S.J.; Khalaj, A.; Noaparast, Z.; Abedi, S.M.; Sabzevari, O. 99mTc-Radiolabeled GE11-M odified Peptide for Ovarian Tumor Targeting. DARU 2017, 25, 13.
8. Chokkappan, K.; Kannivelu, A.; Srinivasan, S.; Babu, S. Review of Diagnostic Uses of Shunt Fraction Quantification wit h Technetium-99m Macroaggregated Albumin 20 Perfusion Scan as Illustrated by a Case of Osler-Weber-Rendu Syndr ome. Ann. Thorac. Med. 2016, 11, 155.
9. Hope, T.A.; Calais, J.; Zhang, L.; Dieckmann, W.; Millo, C. 111In-Pentetreotide Scintigraphy versus 68Ga-Dotatate Pet: Impact on Krenning Scores and Effect of Tumor Burden. J. Nucl. Med. 2019, 60, 1266–1269.
10. Rosenkranz, A.A.; Slastnikova, T.A.; Karmakova, T.A.; Vorontsova, M.S.; Morozova, N.B.; Petriev, V.M.; Abrosimov, A. S.; Khramtsov, Y.V.; Lupanova, T.N.; Ulasov, A.V.; et al. Antitumor Activity of Auger Electron Emitter 111In Delivered by Modular Nanotransporter for Treatment of Bladder Cancer with EGFR Overexpression. Front. Pharmacol. 2018, 9, 133 1.
11. Lütje, S.; Van Rij, C.M.; Franssen, G.M.; Fracasso, G.; Helfrich, W.; Eek, A.; Oyen, W.J.; Colombatti, M.; Boerman, O. C. Targeting Human Prostate Cancer with 111In-Labeled D2B IgG, F (Ab′) 2 and Fab Fragments in Nude Mice with PS MA-Expressing Xenografts. Contrast Media Mol. Imaging 2015, 10, 28–36.
12. Sörensen, J.; Sandberg, D.; Sandström, M.; Wennborg, A.; Feldwisch, J.; Tolmachev, V.; Åström, G.; Lubberink, M.; Ga rske-Román, U.; Carlsson, J.; et al. First-in-Human Molecular Imaging of HER2 Expression in Breast Cancer Metastas es Using the 111In-ABY-025 Affibody Molecule. J. Nucl. Med. 2014, 55, 730–735.

13. Tahara, N.; Zandbergen, H.R.; de Haas, H.J.; Petrov, A.; Pandurangi, R.; Yamaki, T.; Zhou, J.; Imaizumi, T.; Slart, R.H. J.A.; Dyszlewski, M.; et al. Noninvasive Molecular Imaging of Cell Death in Myocardial Infarction Using 111In-GSAO. Sci. Rep. 2014, 4, 6826.

14. Jacobson, O.; Kiesewetter, D.O.; Chen, X. Fluorine-18 Radiochemistry, Labeling Strategies and Synthetic Routes. Bioconjugate Chem. 2015, 26, 1–18.

15. Koç, Z.P.; Kara, P.Ö.; Dağtekin, A. Detection of unknown primary tumor in patients presented with brain metastasis by F-18 fluorodeoxyglucose positron emission tomography/computed tomography. CNS Oncol. 2018, 7, CNS12.

16. Antoni, G. The Radiopharmaceutical Chemistry of Carbon-11: Basic Principles. In Radiopharmaceutical Chemistry; Springer International Publishing: Cham, Switzerland, 2019; pp. 207–220.

17. Goud, N.S.; Bhattacharya, A.; Joshi, R.K.; Nagaraj, C.; Bharath, R.D.; Kumar, P. Carbon-11: Radiochemistry and Target-Based PET Molecular Imaging Applications in Oncology, Cardiology, and Neurology. J. Med. Chem. 2021, 64, 1223–1259.

18. Zheng, Y.; Zhou, Z. SPECT and PET in Vascular Dementia. In PET and SPECT in Neurology; Springer: Cham, Switzerland, 2021; pp. 563–575.

19. Apple, M.; Waksman, R.; Chan, R.C.; Vodovotz, Y.; Fournadjiev, J.; Bass, B.G. Radioactive 133-Xenon Gas-Filled Balloon to Prevent Restenosis: Dosimetry, Efficacy, and Safety Considerations: Dosimetry, Efficacy, and Safety Considerations. Circulation 2002, 106, 725–729.

20. Mettler, F.A.; Guiberteau, M.J. Essentials of Nuclear Medicine Imaging: Expert Consult—Online and Print; W B Saunders: London, UK, 2012.

21. Korell, J.; Coulter, C.V.; Duffull, S.B. Evaluation of Red Blood Cell Labelling Methods Based on a Statistical Model for Red Blood Cell Survival. J. Theor. Biol. 2011, 291, 88–98.

22. Frei, R.; Gaucher, C.; Poulton, S.W.; Canfield, D.E. Fluctuations in Precambrian Atmospheric Oxygenation Recorded by Chromium Isotopes. Nature 2009, 461, 250–253.

23. Ferreira, C.L.; Lamsa, E.; Woods, M.; Duan, Y.; Fernando, P.; Bensimon, C.; Kordos, M.; Guenther, K.; Jurek, P.; Kiefer, G.E. Evaluation of Bifunctional Chelates for the Development of Gallium-Based Radiopharmaceuticals. Bioconjugate Chem. 2010, 21, 531–536.

24. Al-Suqri, B.; Al-Bulushi, N. Gallium-67 Scintigraphy in the Era of Positron Emission Tomography and Computed Tomography: Tertiary Centre Experience. Sultan Qaboos Univ. Med. J. 2015, 15, e338–e343.

25. Othman, M.F.B.; Verger, E.; Costa, I.; Tanapirakgul, M.; Cooper, M.S.; Imberti, C.; Lewington, V.J.; Blower, P.J.; Terry, S.Y.A. In Vitro Cytotoxicity of Auger Electron-Emitting Ga-Trastuzumab. Nucl. Med. Biol. 2020, 80–81, 57–64.

26. Velikyan, I. 68Ga-Based Radiopharmaceuticals: Production and Application Relationship. Molecules 2015, 20, 12913–12943.

27. Meisenheimer, M.; Saenko, Y.; Eppard, E. Gallium-68: Radiolabeling of Radiopharmaceuticals for PET Imaging—A Lot to Consider. In Medical Isotopes; IntechOpen: London, UK, 2021.

28. Frigerio, B.; Franssen, G.; Luison, E.; Satta, A.; Seregni, E.; Colombatti, M.; Fracasso, G.; Valdagni, R.; Mezzanzanica, D.; Boerman, O.; et al. Full Preclinical Validation of the 123I-Labeled Anti-PSMA Antibody Fragment ScFvD2B for Prostate Cancer Imaging. Oncotarget 2017, 8, 10919–10930.

29. Bajaj, N.; Hauser, R.A.; Seibyl, J.; Kupsch, A.; Plotkin, M.; Chen, C.; Grachev, I.D. Association between Hoehn and Yahr, Mini-Mental State Examination, Age, and Clinical Syndrome Predominance and Diagnostic Effectiveness of Ioflupane I 123 Injection (DaTSCANTM) in Subjects with Clinically Uncertain Parkinsonian Syndromes. Alzheimer's Res. Ther. 2014, 6, 67.

30. Stevens, L.A.; Claybon, M.A.; Schmid, C.H.; Chen, J.; Horio, M.; Imai, E.; Nelson, R.G.; Van Deventer, M.; Wang, H.-Y.; Zuo, L.; et al. Evaluation of the Chronic Kidney Disease Epidemiology Collaboration Equation for Estimating the Glomerular Filtration Rate in Multiple Ethnicities. Kidney Int. 2011, 79, 555–562.

31. Schwarz, S.B.; Thon, N.; Nikolajek, K.; Niyazi, M.; Tonn, J.C.; Belka, C.; Kreth, F.W. Iodine-125 Brachytherapy for Brain Tumours-a Review. Radiat. Oncol. 2012, 7, 30.

32. Binder, C.; Mruthyunjaya, P.; Schefler, A.C.; Seider, M.I.; Crilly, R.; Hung, A.; Meltsner, S.; Mowery, Y.; Kirsch, D.G.; Teh, B.S.; et al. Practice Patterns for the Treatment of Uveal Melanoma with Iodine-125 Plaque Brachytherapy: Ocular Oncology Study Consortium Report 5. Ocul. Oncol. Pathol. 2020, 6, 210–218.

33. Suchorska, B.; Hamisch, C.; Treuer, H.; Mahnkopf, K.; Lehrke, R.E.; Kocher, M.; Ruge, M.I.; Voges, J. Stereotactic Brachytherapy Using Iodine 125 Seeds for the Treatment of Primary and Recurrent Anaplastic Glioma WHO III. J. Neurooncol. 2016, 130, 123–131.

34. Drozdovitch, V.; Brill, A.B.; Callahan, R.J.; Clanton, J.A.; DePietro, A.; Goldsmith, S.J.; Greenspan, B.S.; Gross, M.D.; Hays, M.T.; Moore, S.C.; et al. Use of Radiopharmaceuticals in Diagnostic Nuclear Medicine in the United States: 1960–2010. Health Phys. 2015, 108, 520–537.

35. Dorbala, S.; Hachamovitch, R.; Curillova, Z.; Thomas, D.; Vangala, D.; Kwong, R.Y.; Di Carli, M.F. Incremental Prognostic Value of Gated Rb-82 Positron Emission Tomography Myocardial Perfusion Imaging over Clinical Variables and Rest LVEF. JACC Cardiovasc. Imaging 2009, 2, 846–854.

36. Kostenikov, N.A.; Zhuikov, B.L.; Chudakov, V.M.; Iliuschenko, Y.R.; Shatik, S.V.; Zaitsev, V.V.; Sysoev, D.S.; Stanzhevskiy, A.A. Application of 82 Sr/82 Rb Generator in Neurooncology. Brain Behav. 2019, 9, e01212.

37. Fathala, A.; Aboulkheir, M.; Shoukri, M.M.; Alsergani, H. Diagnostic Accuracy of 13N-Ammonia Myocardial Perfusion Imaging with PET-CT in the Detection of Coronary Artery Disease. Cardiovasc. Diagn. Ther. 2019, 9, 35–42.

38. Vente, M.A.; Wit, T.C.; Van Den Bosch, M.A.; Bult, W.; Seevinck, P.R.; Zonnenberg, B.A. Holmium-166 Poly (L-Lactic Acid) Microsphere Radioembolization of the Liver: Technical Aspects Studied in a Large Animal Model. Eur. Radiol. 2010, 20, 862–869.

39. Mishiro, K.; Hanaoka, H.; Yamaguchi, A.; Ogawa, K. Radiotheranostics with Radiolanthanides: Design, Development Strategies, and Medical Applications. Coord. Chem. Rev. 2019, 383, 104–131.

40. Watering, F.C.J.; Rijpkema, M.; Perk, L.; Brinkmann, U.; Oyen, W.J.G.; Boerman, O.C. Zirconium-89 Labeled Antibodies: A New Tool for Molecular Imaging in Cancer Patients. BioMed Res. Int. 2014, 2014, 203601.

41. Yip, C.; Blower, P.J.; Goh, V.; Landau, D.B.; Cook, G.J.R. Molecular Imaging of Hypoxia in Non-Small-Cell Lung Cancer. Eur. J. Nucl. Med. Mol. Imaging 2015, 42, 956–976.

42. Fodero-Tavoletti, M.T.; Villemagne, V.L.; Paterson, B.M.; White, A.R.; Li, Q.-X.; Camakaris, J.; O'Keefe, G.; Cappai, R.; Barnham, K.J.; Donnelly, P.S. Bis(Thiosemicarbazonato) Cu-64 Complexes for Positron Emission Tomography Imaging of Alzheimer's Disease. J. Alzheimers Dis. 2010, 20, 49–55.

43. Niccoli Asabella, A.; Cascini, G.L.; Altini, C.; Paparella, D.; Notaristefano, A.; Rubini, G. The Copper Radioisotopes: A Systematic Review with Special Interest to 64Cu. Biomed Res. Int. 2014, 2014, 786463.

44. Cohen, I.; Robles, A.; Mendoza, P.; Airas, R.; Montoya, E. Experimental Evidences of 95mTc Production in a Nuclear Reactor. Appl. Radiat. Isot. 2018, 135, 207–211.

45. Costa, I.M.; Siksek, N.; Volpe, A.; Man, F.; Osytek, K.M.; Verger, E.; Schettino, G.; Fruhwirth, G.O.; Terry, S.Y.A. Relationship of in Vitro Toxicity of Technetium-99m to Subcellular Localisation and Absorbed Dose. Int. J. Mol. Sci. 2021, 22, 13466.

46. Qin, H.; Shao, W. The Recent Research Progress on 99 Mo/99 Tc m Generator. Labeled Immunoass. Clin. Med. 2016, 23, 949–953.

47. Rathmann, S.M.; Ahmad, Z.; Slikboer, S.; Bilton, H.A.; Snider, D.P.; Valliant, J.F. The Radiopharmaceutical Chemistry of Technetium-99m. In Radiopharmaceutical Chemistry; Springer International Publishing: Cham, Switzerland, 2019; pp. 311–333.

48. Alberto, R. From Oxo to Carbonyl and Arene Complexes; A Journey through Technetium Chemistry. J. Organomet. Chem. 2018, 869, 264–269.

49. Qaiser, S.; Khan, A.; Khan, M. Synthesis, Biodistribution and Evaluation of 99m Tc-Sitafloxacin Kit: A Novel Infection Imaging Agent. J. Radioanal. Nucl. Chem. 2010, 284, 189–193.

50. Herrero Álvarez, N.; Bauer, D.; Hernández-Gil, J.; Lewis, J.S. Recent Advances in Radiometals for Combined Imaging and Therapy in Cancer. ChemMedChem 2021, 16, 2909–2941.

51. Terova, O.S. Characterization and Inertness Studies of Gallium (III) and Indium (III) Complexes of Dicarboxymethyl Pendantarmed Cross-Bridged Cyclam; University of New Hampshire: Durham, NH, USA, 2008.

52. Spang, P.; Herrmann, C.; Roesch, F. Bifunctional Gallium-68 Chelators: Past, Present, and Future. Semin. Nucl. Med. 2016, 46, 373–394.

53. Fani, M.; André, J.P.; Maecke, H.R. 68Ga-PET: A Powerful Generator-Based Alternative to Cyclotron-Based PET Radiopharmaceuticals. Contrast Media Mol. Imaging 2008, 3, 67–77.

54. Rahmim, A.; Zaidi, H. PET versus SPECT: Strengths, Limitations and Challenges. Nucl. Med. Commun. 2008, 29, 193–207.

55. Shetty, D.; Lee, Y.-S.; Jeong, J.M. (68)Ga-Labeled Radiopharmaceuticals for Positron Emission Tomography. Nucl. Med. Mol. Imaging 2010, 44, 233–240.

56. Kostelnik, T.I.; Orvig, C. Radioactive Main Group and Rare Earth Metals for Imaging and Therapy. Chem. Rev. 2018, 119, 902–956.

57. Bin Othman, M.F.; Mitry, N.R.; Lewington, V.J.; Blower, P.J.; Terry, S.Y. Re-Assessing Gallium-67 as a Therapeutic Radionuclide. Nucl. Med. Biol. 2017, 46, 12–18.

58. de Andrade Martins, P.; Osso, J.A., Jr. Thermal Diffusion of 67Ga from Irradiated Zn Targets. Appl. Radiat. Isot. 2013, 82, 279–282.

59. Meulen, N.P.; Dolley, S.G.; Steyn, G.F.; Walt, T.N.; Raubenheimer, H.G. The Use of Selective Volatization in the Separation of 68Ge from Irradiated Ga Targets. Appl. Radiat. Isot. 2011, 69, 727–731.

60. Velikyan, I. Prospective of 68Ga-Radiopharmaceutical Development. Theranostics 2013, 4, 47–80.

61. Prata, I.M. Gallium-68: A New Trend in PET Radiopharmacy. Curr. Radiopharm. 2012, 5, 142–149.

62. Blower, J.E.; Cooper, M.S.; Imberti, C.; Ma, M.T.; Marshall, C.; Young, J.D.; Blower, P.J. The Radiopharmaceutical Chemistry of the Radionuclides of Gallium and Indium. In Radiopharmaceutical Chemistry; Springer: Cham, Switzerland, 2019; pp. 255–271.

63. Khosravifarsani, M.; Ait-Mohand, S.; Paquette, B.; Sanche, L.; Guérin, B. Design, Synthesis, and Cytotoxicity Assessment of Cu-NOTA-Terpyridine Platinum Conjugate: A Novel Chemoradiotherapeutic Agent with Flexible Linker. Nanomaterials 2021, 11, 2154.

64. Wu, N.; Kang, C.S.; Sin, I.; Ren, S.; Liu, D.; Ruthengael, V.C.; Lewis, M.R.; Chong, H.-S. Promising Bifunctional Chelators for Copper 64-PET Imaging: Practical (64)Cu Radiolabeling and High in Vitro and in Vivo Complex Stability. J. Biol. Inorg. Chem. 2016, 21, 177–184.

65. Pichler, V.; Berroterán-Infante, N.; Philippe, C.; Vraka, C.; Klebermass, E.-M.; Balber, T.; Pfaff, S.; Nics, L.; Mitterhauser, M.; Wadsak, W. An Overview of PET Radiochemistry, Part 1: The Covalent Labels 18F, 11C, and 13N. J. Nucl. Med. 2018, 59, 1350–1354.

66. Archibald, S.J.; Allott, L. The Aluminium-Fluoride Revolution: Simple Radiochemistry with a Big Impact for Radiolabelled Biomolecules. EJNMMI Radiopharm. Chem. 2021, 6, 30.

67. Cieslak, J.A.; Sibenaller, Z.A.; Walsh, S.A.; Ponto, L.L.B.; Du, J.; Sunderland, J.J.; Cullen, J.J. Fluorine-18-Labeled Thymidine Positron Emission Tomography (FLT-PET) as an Index of Cell Proliferation after Pharmacological Ascorbate-Based Therapy. Radiat. Res. 2016, 185, 31–38.

68. McBride, W.J.; D'Souza, C.A.; Sharkey, R.M.; Karacay, H.; Rossi, E.A.; Chang, C.-H.; Goldenberg, D.M. Improved 18F labeling of peptides with a fluoride-aluminum-chelate complex. Bioconjugate Chem. 2010, 21, 1331–1340.

69. Deng, X.; Rong, J.; Wang, L.; Vasdev, N.; Zhang, L.; Josephson, L.; Liang, S.H. Chemistry for Positron Emission Tomography: Recent Advances in 11 C-, 18 F-, 13 N-, and 15 O-Labeling Reactions. Angew. Chem. Int. Ed. 2019, 58, 2580–2605.

70. Ramogida, C.F.; Orvig, C. Tumour Targeting with Radiometals for Diagnosis and Therapy. Chem. Commun. 2013, 49, 4720–4739.

71. Tickner, B.J.; Stasiuk, G.J.; Duckett, S.B.; Angelovski, G. The Use of Yttrium in Medical Imaging and Therapy: Historical Background and Future Perspectives. Chem. Soc. Rev. 2020, 49, 6169–6185.

72. Das, T.; Pillai, M.R.A. Options to Meet the Future Global Demand of Radionuclides for Radionuclide Therapy. Nucl. Med. Biol. 2013, 40, 23–32.

73. Tong, A.K.T.; Kao, Y.H.; Too, C.W.; Chin, K.F.W.; Ng, D.C.E.; Chow, P.K.H. Yttrium-90 Hepatic Radioembolization: Clinical Review and Current Techniques in Interventional Radiology and Personalized Dosimetry. Br. J. Radiol. 2016, 89, 20150943.

74. Sciacca, F. Samarium-153. 2020. Available online: https://radiopaedia.org/articles/samarium-153 (accessed on 24 April 2021).

75. Kasbollah, A.; Amiroudine, M.Z.A.M.; Karim, J.A.; Hamid, S.S.A.; Ghazi, S.A.F.W.S.M.; Awang, W.A.W.; Ali, M.R. Samarium-153 Production Using (n,γ) Reaction at Triga Puspati Research Reactor. In Application of Mathematics in Technical and Natural Sciences: Proceedings of the 12th International On-line Conference for Promoting the Application of Mathematics in Technical and Natural Sciences—AMiTaNS'20; AIP Publishing: Melville, NY, USA, 2020.

76. Scheinberg, D.A.; McDevitt, M.R. Actinium-225 in Targeted Alpha-Particle Therapeutic Applications. Curr. Radiopharm. 2011, 4, 306–320.

77. Gupta, N.; Devgan, A.; Bansal, I.; Olsavsky, T.D.; Li, S.; Abdelbaki, A.; Kumar, Y. Usefulness of Radium-223 in Patients with Bone Metastases. Proc. Bayl. Univ. Med. Cent. 2017, 30, 424–426.

78. Argyrou, M.; Valassi, A.; Andreou, M.; Lyra, M. Rhenium-188 Production in Hospitals, by W-188/Re-188 Generator, for Easy Use in Radionuclide Therapy. Int. J. Mol. Imaging 2013, 2013, 290750.

79. Lepareur, N.; Lacœuille, F.; Bouvry, C.; Hindré, F.; Garcion, E.; Chérel, M.; Noiret, N.; Garin, E.; Knapp, F.F.R., Jr. Rhenium-188 Labeled Radiopharmaceuticals: Current Clinical Applications in Oncology and Promising Perspectives. Front. Med. 2019, 6, 132.
80. Wick, R.R.; Nekolla, E.A.; Gaubitz, M.; Schulte, T.L. Increased Risk of Myeloid Leukaemia in Patients with Ankylosing Spondylitis Following Treatment with Radium-224. Rheumatology 2008, 47, 855–859.
81. Piotrowska, A.; Leszczuk, E.; Bruchertseifer, F.; Morgenstern, A.; Bilewicz, A. Functionalized NaA Nanozeolites Labeled with (224,225)Ra for Targeted Alpha Therapy. J. Nanoparticle Res. 2013, 15, 2082.
82. Cordier, D.; Forrer, F.; Bruchertseifer, F.; Morgenstern, A.; Apostolidis, C.; Good, S.; Müller-Brand, J.; Mäcke, H.; Reubi, J.C.; Merlo, A. Targeted Alpha-Radionuclide Therapy of Functionally Critically Located Gliomas with 213Bi-DOTA--Substance P: A Pilot Trial. Eur. J. Nucl. Med. Mol. Imaging 2010, 37, 1335–1344.
83. Wright, C.L.; Zhang, J.; Tweedle, M.F.; Knopp, M.V.; Hall, N.C. Theranostic Imaging of Yttrium-90. BioMed Res. Int. 2015, 2015, 481279.
84. Goffredo, V.; Paradiso, A.; Ranieri, G.; Gadaleta, C.D. Yttrium-90 (90Y) in the Principal Radionuclide Therapies: An Efficacy Correlation between Peptide Receptor Radionuclide Therapy, Radioimmunotherapy and Transarterial Radioembolization Therapy. Ten Years of Experience (1999–2009). Crit. Rev. Oncol. Hematol. 2011, 80, 393–410.
85. Rösch, F.; Herzog, H.; Qaim, S.M. The Beginning and Development of the Theranostic Approach in Nuclear Medicine, as Exemplified by the Radionuclide Pair 86Y and 90Y. Pharmaceuticals 2017, 10, 56.
86. Kam, B.L.R.; Teunissen, J.J.M.; Krenning, E.P.; de Herder, W.W.; Khan, S.; van Vliet, E.I.; Kwekkeboom, D.J. Lutetium-Labelled Peptides for Therapy of Neuroendocrine Tumours. Eur. J. Nucl. Med. Mol. Imaging 2012, 39 (Suppl. S1), S103–S112.
87. Rahbar, K.; Ahmadzadehfar, H.; Kratochwil, C.; Haberkorn, U.; Schaefers, M.; Essler, M.; Krause, B.J. German Multicenter Study Investigating Lu-177-PSMA-617 Radioligand Therapy in Advanced Prostate Cancer Patients. J. Nucl. Med. 2017, 58, 85–90.
88. Bober, B.; Saracyn, M.; Zaręba, K.; Lubas, A.; Mazurkiewicz, P.; Wilińska, E.; Kamiński, G. Early Complications of Radioisotope Therapy with Lutetium-177 and Yttrium-90 in Patients with Neuroendocrine Neoplasms-A Preliminary Study. J. Clin. Med. 2022, 11, 919.
89. Dash, A.; Pillai, M.R.A.; Knapp, F.F., Jr. Production of (177)Lu for Targeted Radionuclide Therapy: Available Options. Nucl. Med. Mol. Imaging 2015, 49, 85–107.
90. Banerjee, S.; Pillai, M.R.A.; Knapp, F.F.R. Lutetium-177 Therapeutic Radiopharmaceuticals: Linking Chemistry, Radiochemistry, and Practical Applications. Chem. Rev. 2015, 115, 2934–2974.

Retrieved from https://encyclopedia.pub/entry/history/show/56081